Desalination and Water Treatment
www.deswater.com

doi: 10.5004/dwt.2021.27683

236 (2021) 108–122
October

Adsorption of silver, thorium and nickel ions from aqueous solution onto rice husk

Shagufta Zafar[a,†], Muhammad Imran Khan[b,*,†], Abdallah Shanableh[b], Saleem Ahmad[c], Suryyia Manzoor[d], Shabnam Shahida[e], Prasert Prapamonthon[f], Sidra Mubeen[g,*], Aziz ur Rehman[h]

[a]*Department of Chemistry, The Government Sadiq College Women University, Bahawalpur 63000, Pakistan, email: shg_zf@gscwu.edu.pk*
[b]*Research Institute of Sciences and Engineering, University of Sharjah, Sharjah 27272, United Arab Emirates, email: raoimranishaq@gmail.com/mimran@sharjah.ac.ae ((M. Imran Khan), shanableh@sharjah.ac.ae (A. Shanableh)*
[c]*Shantou University Medical College, Cancer Hospital Shantou, Guangdong 515041, P.R. China, email: ahmad.chilas@gmail.com*
[d]*Institute of Chemical Sciences, Bahauddin Zakariya University, Multan 60800, Pakistan, email: suryyia.manzoor@bzu.edu.pk*
[e]*Department of Chemistry, University of Poonch, Rawalakot 12350, Azad Kashmir, Pakistan, email: shabnamshahida01@gmail.com*
[f]*King Mongkut's Institute of Technology Ladkrabang, Bangkok, Thailand, email: prasert.pr@kmitl.ac.th*
[g]*Department of Chemistry, The Women University Multan, Katchery Campus, LMQ Road, Multan, email: sidra_sidra786@yahoo.com*
[h]*Institute of Chemistry, Baghdad-ul-Jadeed Campus, The Islamia University of Bahawalpur, Bahawalpur 63100, Pakistan, email: azizypk@yahoo.com*

Received 27 March 2021; Accepted 4 August 2021

ABSTRACT

In this article, adsorption of metal ions such as silver (Ag(I)), thorium (Th(IV)) and nickel (Ni(II)) from aqueous solution onto rice husk (RH) was performed at room temperature. Adsorption of these metal ions (silver, thorium, and nickel) onto RH was demonstrated by using Fourier transform infrared spectroscopy and energy-dispersive X-ray. Morphology of RH was investigated before and after adsorption of these metal ions onto it by using scanning electron microscopy. The effect of different operational parameters (contact time, initial concentration of metal ion solution, weight of RH, pH, and temperature) on the percentage removal of these metal ions was explored in detail and compared. Experimental data for adsorption of these metal ions onto RH was subjected to Langmuir and Freundlich isotherm models. Results showed that adsorption of silver and thorium fitted well to Langmuir isotherm model ($R^2 > 0.99$) whereas adsorption of Ni(II) fitted well to Freundlich isotherm model ($R^2 > 0.99$). Adsorption kinetics study demonstrated that adsorption of these metal ions onto RH from aqueous solution fitted well to pseudo-second-order model. Adsorption thermodynamics investigation represented that adsorption of these metal ions onto RH was endothermic process. The values of Gibb's free energy were –6.53 to –9.17 kJ/mol for Ag(I), –1.11 to –3.57 kJ/mol for Th(IV) and –0.89 to –1.40 kJ/mol for Ni(II). The negative values of Gibb's free energy for these metal ions suggested that the adsorption process was spontaneous in nature. The regeneration of RH and recovery of these metal ions were also studied.

Keywords: Metal ions; Adsorption; Endothermic process; Rice husk; Adsorption kinetics

* Corresponding authors.
† Both authors contributed equally to this work.

1. Introduction

Particularly in developing countries, heavy metal pollution is a global environmental issue, which is resulted from the enhancement of agricultural and industrial activities as well as the improper removal of metal ions from domestic and wastewater effluents [1,2]. Industrial sources, smelters and foundries, combustion by-products, the paint industry and automobiles are the main sources of heavy metals pollution in aqueous systems. It results in serious health issues, especially to the immune systems and human central nervous [3]. To solve this issue, researchers have fascinated their interests in heavy metal treatment by removing or at least decreasing their concentrations to acceptable levels according to government regulations [4]. Herein, the representative heavy metals are silver (Ag(I)), thorium (Th(IV)) and nickel (Ni(II)). They are harmful to both human beings and animals. The removal of these heavy metals from wastewater is crucial for life and the environment.

Over the past few decades, several methods including adsorption [5,6], oxidation, chemical precipitation, flocculation [7], membrane filtration [8], catalytic degradation, electrolysis, and biodegradation were utilized for the removal of poisonous heavy metals [9–11]. Nevertheless, these technologies have their own prejudices, including expensive, long time-consuming, sensitivity to the environment and ambitious for operation. These issues limit their practical uses in the discharge of metal ions from wastewaters. Adsorption is generally endorsed in terms of its cost-effectiveness, environmental friendliness, simplicity in handling and high efficiency among methods used for segregate toxic heavy metals [12,13].

A lot of materials including activated carbons [14], carbon nanotubes [15], zeolites [16], chitosan [17], clays [18] and agricultural wastes [19] were used to remove metal cations from aqueous solutions. After all, there were still few drawbacks that obligated their practical applications such as the adsorption capacity of these adsorbents is not enough, these adsorbents are difficult to isolate, and so on [20,21]. Therefore, it is crucial to find out a new adsorbent. Presently, the utilization of agro-wastes as adsorbents is attracting great interest because of their cheapness, presence in large quantity, the existence of porous morphology and relatively high fixed carbon content.

Pakistan is a rice-producing country in Asia and provides rice husk (RH) as agricultural waste material. The annual rice production worldwide is approximately 500 million metric tons of which 10%–20% is RH [22,23]. About 70%–85% of organic matter is present in RH, which possesses sugars, cellulose and lignin, etc., while silica is also present in the cellular membrane [23,24]. It postures a disposal issue for the mill owners. Previously, we studied the adsorption of several metal ions onto RH via batch model at room temperature [20,25,26]. In this article, the removal of metal ions including silver, thorium and nickel from aqueous solution by RH was reported via batch mode. The effect of operating factors (contact time, weight of RH, initial concentration of metal ions solution, temperature and pH) on the percentage removal of these metal ions from aqueous solution was explored under constant conditions and compared with each other. Adsorption isotherms, kinetics, and thermodynamics for adsorption of these metal ions onto RH were also investigated. Moreover, the regeneration of RH (adsorbent) and recovery of these metal ions was also explored.

2. Experimental

2.1. Materials

All the chemicals used during this research were of analytical grade and used as received. The temperature of the solution was restrained by soaking the culture tube in a water bath of Gallenkamp Thermostirrer (UK) for thermodynamic evaluation. Deionized water was used throughout the work. The fidelity of the temperature in the water bath was ±0.1°C.

2.2. Adsorbent

Rice husk (RH) of basmati rice was kindly provided by rice mills of Punjab, Pakistan (Fig. S1). To remove dust particles, RH was thoroughly washed with water and then dried at 80°C. It was stored in a pre-cleaned airtight container and was employed without any more physical or chemical pre-treatment. Its chemical analysis for their trace metal contents was performed by atomic adsorption spectrometry (AAS) and neutron activation analysis (NAA). Results represented that the concentration of metals namely Na, K, Pb and Fe was present in μg/g of sample. Silica contents were 18.27 (0.62%) of RH. The small concentration of elements in RH was demonstrated by standard procedures.

2.3. Adsorption of silver, thorium and nickel onto RH

Adsorption of silver, thorium and nickel ions onto RH was carried out as described [20,25–28] (Section S1 – Adsorption of silver, thorium and nickel onto rice husk).

2.4. Characterization

2.4.1. Instrumentation

Detail instrumentation studies, for example, Fourier transform infrared (FTIR) spectrometer (Vector 22, Bruker), field emission scanning electron microscope (FE-SEM, SIRION 200, FEI Company, USA), and energy-dispersive X-ray (EDX) analysis were employed (Section S2 – Instrumentations).

2.5. Adsorption equilibrium

Adsorption equilibrium was explored by using Langmuir and Freundlich adsorption isotherms (Section S3 – Adsorption equilibrium).

2.6. Adsorption kinetics

Adsorption kinetics for silver, thorium and nickel ions was studied by using pseudo-first-order and pseudo-second-order models (Section S4 – Adsorption kinetics).

2.7. Adsorption thermodynamics

Adsorption thermodynamics for adsorption of silver, thorium and nickel ions onto RH was also evaluated. The values of change in Gibb's free energy (ΔG°), enthalpy (Δ*H*°) and entropy (Δ*S*°) were calculated by employing the below relationships:

$$\ln K_c = \frac{\Delta S^\circ}{R} - \frac{\Delta H^\circ}{RT} \quad (1)$$

$$K_c = \frac{C_a}{C_e} \quad (2)$$

$$\Delta G^\circ = \Delta H^\circ - T\Delta S^\circ \quad (3)$$

where K_c, ΔG°, ΔH° and ΔS° are denoting equilibrium constant, change in Gibb's free energy (kJ/mol), enthalpy (kJ/mol) and entropy (J/mol K) respectively.

3. Results and discussion

3.1. Morphology

Morphology of virgin RH and metal ions (Ag(I), Th(IV) and Ni(II)) load RH was studied by using field emission scanning electron microscopy (FE-SEM) as described [29,30]. Fig. S2 shows FE-SEM images of virgin RH and metal ions (Ag(I), Th(IV) and Ni(II)) loaded RH. Results indicated that the surface roughness of RH was modified significantly after the adsorption of these metal ions onto it. The pores and groves were filled which were present before metal ions adsorption and a decrease in surface heterogeneity was observed resulting in the smooth surface of RH. Ionic radii of silver and nickel are 0.129 and 0.074 nm, respectively, which are much smaller than the pore size present on RH, (100–180 nm), enabling adsorption of these metal ions through pore diffusion. It resulted to change in the surface of RH to a smooth one.

3.2. FTIR and EDX tests

Herein, the adsorption of these metal ions on RH was confirmed by FTIR spectroscopy as described by researchers [31–34]. Fig. S3 denotes the FTIR spectrum of virgin RH. The peaks at 1,217.0; 1,365.4; 1,737.8 and 1,027.4 cm^{-1} were associated to carboxyl group on RH in range of reported peaks at 1,208–1,230; 1,367–1,371; 1,740 and 1,029 cm^{-1} for carboxyl group [35,36]. The characteristic absorption band at 3,400–3,200 cm^{-1} was attributed for surface O–H stretching whereas aliphatic C–H stretching had a broadband at 2,921–2,851 cm^{-1}. The peaks at 1,737.8; 1,435.6 and 1,365.4 cm^{-1} were attributed with C=O stretching, OH bending of adsorbed H_2O and aliphatic C–H bending respectively [37]. Further, the peak at 1,074.0 cm^{-1} was due to the anti-symmetric stretching vibration of Si–O, whereas at 476.2 cm^{-1} indicated the bending vibration of the Si–O–Si bond [35,38,39].

After adsorption of Ag(I), Th(IV) and Ni(II) onto RH, FTIR spectrum indicated the changes in the functional groups intensity or position, responsible for metal ions adsorption (Fig. S3). FTIR spectrum of Ag(I) loaded RH represents shifting of peaks to 2,921.6; 1,634.3 and 1,506.1 cm^{-1}. For Ni(II) loaded RH, the peaks shifted to 2,910.1; 1,734.7, 1,646.8 and 1,372.8 cm^{-1}, whereas intensities of 1,734.7; 1,216.3 and 1,027.7 cm^{-1} were observed after Ni(II) adsorption onto RH. Following the Th(IV) adsorption, FTIR spectrum of RH exhibited variations in the peak positions and relative intensities. The shifting of peaks to 421.8; 464; 489; 1,035; 1,081; 1,435; 1,739.5 cm^{-1} and the decrease in the intensities of 1,029; 1,093; 1,217 and 1,366.8 cm^{-1} were noted.

Fig. S4 depicts the EDX images of virgin RH and metal ions (Ag(I), Th(IV), Ni(II)) loaded RH. Adsorption of metal ions (silver, thorium, nickel) onto RH was also demonstrated by the EDX test of metal ions loaded RH. The presence of peak for silver ion in range of 3.00 to 3.50 keV, for thorium ion in range of 2.50 to 3.55 keV and for nickel ion in range of 0.70 to 8.10 keV representing their successful adsorption onto RH.

3.3. Effect of operating factors on percentage discharge of metal ions

The effect of contact time, weight of RH, initial concentration of metal ions solution, temperature and pH were discussed as:

3.3.1. Effect of contact time

Fig. 1a represents the effect of contact time on the percentage removal of Ag(I), Th(IV) and Ni(II) from aqueous solution by RH at ambient temperature. The removal of these metal ions was found to be increased with contact time. With increasing contact time from 0 to 20 min, the percentage removal of Ag(I), Th(IV) and Ni(II) from aqueous solution by using RH was increased at ambient temperature. The percentage removal of Ag(I), Th(IV) and Ni(II) was increased from 73% to 92%, 40% to 68% and 43% to 60% respectively. At the start, it was noted that the removal of these metal ions was rapid from aqueous solution by RH. After that, there was no big enhancement in the percentage removal of these metal ions from the aqueous solution by RH. Then, the equilibrium was attained. The rapid reaction in the start was due to the presence of many vacant sites onto the surface of RH. It results in interaction between metal ions and adsorption sites. After that adsorption of these metal ions was decreased because of their movement into interior pores of RH when all surface sites were covered. The optimized contact time attained for these metal ions was different and used for further study.

3.3.2. Effect of the weight of RH

The effect of the weight of RH on the percentage removal of Ag(I), Th(IV) and Ni(II) from aqueous solution by RH at room temperature is depicted in Fig. 1b. Results showed that the removal of these metal ions from aqueous solution was increased with increasing the weight of RH. The percentage removal of Ag(I), Th(IV) and Ni(II) from aqueous solution by RH was enhanced from 45% to 93%, 50% to 68% and 42% to 64% respectively. Attained optimized

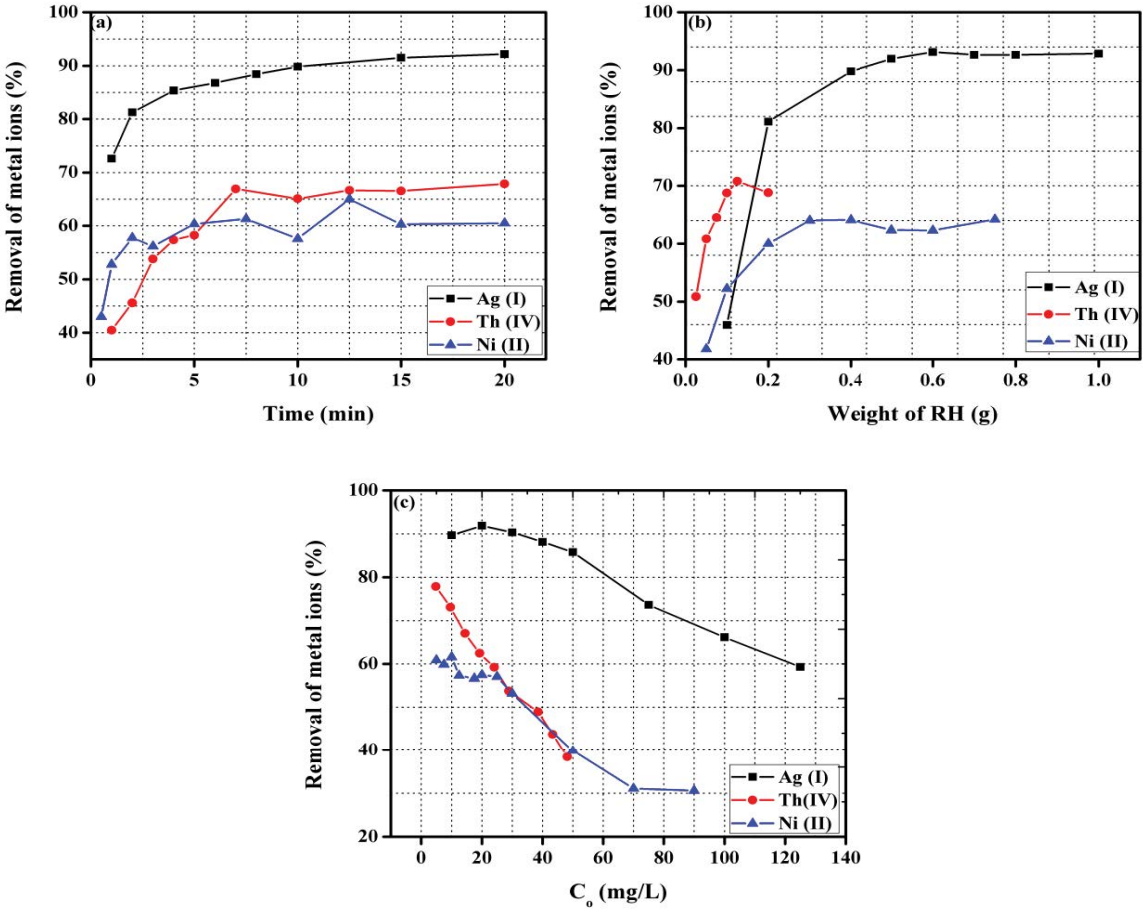

Fig. 1. (a) Effect of contact time (Time = Variable, Volume = 10 mL; Conc. 10 ppm; Weight of RH = 0.5 g for Ag(I); Time = Variable, Volume = 4 mL, Volume of trace = 0.05 mL, Conc. = 24.07 ppm, weight of RH = 0.10 g for Th(IV); Time = Variable, Volume = 10 mL, Conc. = 20.26 ppm, Weight of RH = 0.30 g for Ni(II)), (b) effect of weight of RH (Weight = Variable, Time = 20 min, Volume = 10 mL, Conc. 10 ppm for Ag(I); Weight = Variable, Time = 10 min, Volume = 4 mL, Volume of trace = 0.025 mL, Conc. = 24.07 ppm for Th(IV); Weight = Variable, Time = 30, Volume = 10 mL, Conc. = 20 ppm for Ni(II)), and (c) effect of initial concentration of metal ion solution (Conc. = Variable, Time = 15 min, Volume = 10 mL, Weight of RH = 0.5 g for Ag(I); Conc. = Variable, Time = 20 min, Volume = 4 mL, weight of RH = 0.10 g for Th(IV); Conc. = Variable, Time = 15 min, Volume = 10 mL, Weight of RH = 0.30 g for Ni(II)) on the percentage removal of metal ions from aqueous solution by RH.

weights of RH were 0.5, 0.1 and 0.3 g for Ag(I), Th(IV), Ni(II) respectively. They were used in further research. Similar results were attained in our previous work [20,27].

3.3.3. Effect of initial concentration of metal ions solution

Fig. 1c denotes the effect of the initial concentration of metal ions solution on the percentage removal of Ag(I), Th(IV) and Ni(II) from aqueous solution by RH at ambient temperature. From Fig. 1c it was noted that percentage removal of Ag(I), Th(IV) and Ni(II) from aqueous solution was decreased with increasing initial concentration of metal ions. Some of the metal ions were not adsorbed at a higher initial concentrations of Ag(I), Th(IV) and Ni(II) because of saturation of adsorption sites. At a low concentration of metal ions, there were maximum binding sites between metal ions and RH. With increasing the initial concentration of metal ions solution, the number of ions competing for existing binding sites onto RH was enhanced.

3.3.4. Effect of temperature

It is crucial to investigate the influence of temperature on adsorption of Ag(I), Th(IV) and Ni(II) onto RH from aqueous solution. Fig. 2a represents the effect of temperature on the percentage removal of Ag(I), Th(IV) and Ni(II) from aqueous solution by RH. Attained results showed that the removal of Ag(I), Th(IV) and Ni(II) from aqueous solution by RH was increased with rise in temperature. The removal of Ag(I), Th(IV) and Ni(II) was enhanced from 94% to 96%, 61% to 81% and 60% to 65% respectively with rise in temperature. It was associated to acceleration of some originally slow adsorption steps or to the creation of some new active sites on the surface of RH (adsorbent).

3.3.5. Effect of pH

The pH of the adsorption medium affects the adsorption of Ag(I), Th(IV) and Ni(II) onto different adsorbents and it is a significant factor. The chemical speciation, metal

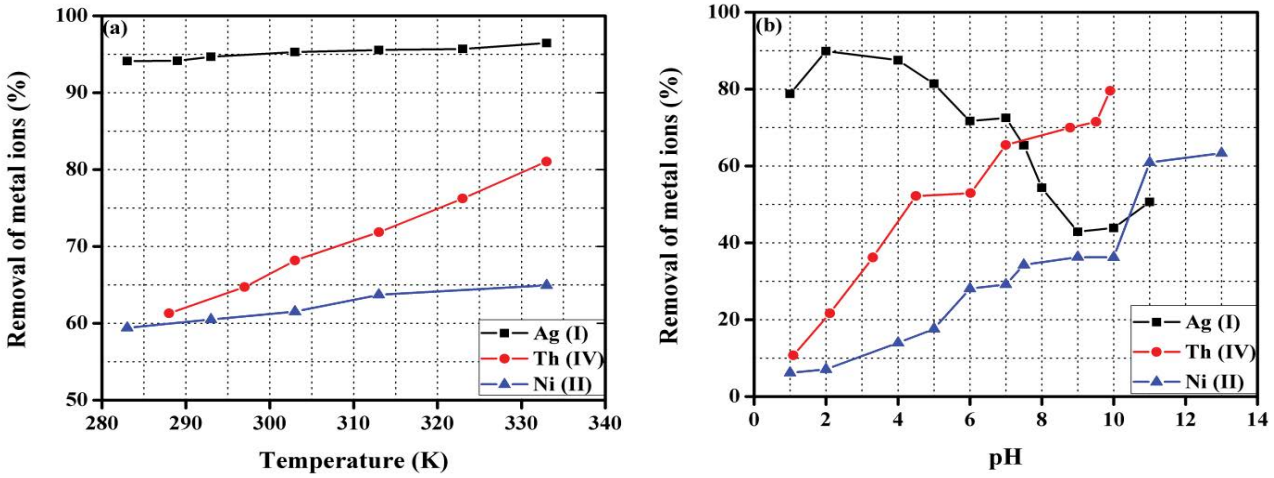

Fig. 2. (a) Effect of temperature (Temperature = Variable, Conc. = 20 ppm, Time = 15 min, Volume = 10 mL, Weight of RH = 0.5 g for Ag(I); Temperature = Variable, Conc. = 12.04 ppm, Time = 20 min, Volume = 4 mL, Weight of RH = 0.10 g for Th(IV); Temperature = Variable, Conc. = 20 ppm, Time = 15 min, Volume = 10 mL, Weight of RH = 0.30 g for Ni(II)) and (b) effect of pH (pH = Variable, Conc. = 10 ppm, Time = 15 min, Volume = 10.10 mL, Weight of RH = 0.5 g for Ag(I); pH = Variable, Volume of traces = 0.025 mL, Conc. = 12.04 ppm, Time = 20 min, Volume = 4 mL, weight of RH = 0.10 g for Th(IV); pH = Variable, Conc. = 20 ppm, Time = 15 min, Volume = 10 mL, Weight of RH = 0.30 g for Ni(II)) on the percentage removal of metal ions from aqueous solution by RH.

ions solubility, and counter ions concentration on the functional groups of the adsorbents were also affected by the pH of adsorbing medium [20]. Herein, the effect of pH on the percentage removal of Ag(I), Th(IV) and Ni(II) from aqueous solution by RH was demonstrated in detail and results are shown in Fig. 2b. It was observed that the percentage removal of Th(IV) and Ni(II) was increased with an increase in pH of the medium at room temperature. From Fig. 2b it is seen that the higher percentage removal of Th(IV) and Ni(II) from aqueous solution by RH took place at pH = 10 and pH = 13 receptively. Adsorption of Th(IV) and Ni(II) onto RH from aqueous solution in basic medium took place on the cellulose part of the RH (adsorbent). It could also be due to the surface complex formation phenomenon with several organic components of the RH [20,40–43]. On the other hand, the percentage removal of Ag(I) from aqueous solution by RH was decreased with an increase in pH of the medium at ambient temperature. The maximum removal of Ag(I) was at pH = 2 from aqueous solution by RH at room temperature. Hence, adsorption of Ag(I) was higher in the acidic medium onto RH from an aqueous solution.

3.4. Adsorption isotherms

Adsorption isotherm curves (C_e vs. q_e) for adsorption of silver, thorium and nickel ions onto RH are represented in Fig. 3. In addition, experimental data for adsorption of silver, thorium and nickel were also subjected to Langmuir and Freundlich isotherms.

Fig. 4 represents Langmuir isotherms for adsorption of these metal ions (silver, thorium and nickel) onto RH and the attained values of isotherm parameters are given in Table 1. The values of correlation coefficient (R^2) for adsorption of silver, thorium and nickel onto RH were 0.992, 0.992 and 0.802 respectively. It showed that the adsorption of silver, thorium and nickel onto RH followed Langmuir's adsorption isotherm. But adsorption of Ag(I) and Th(IV) fitted well to Langmuir adsorption isotherm compared to Ni(II) (R^2 > 0.99). For adsorption of Ag(I), Th(IV) and Ni(II) onto RH, the values of R_L are given in Table 1 which showed the adsorption of these metal ions (silver, thorium and nickel) onto RH was a favorable process.

Fig. 5 depicts Freundlich isotherm for adsorption of silver, thorium and nickel ions onto RH. The value of Freundlich constants (n and K_F) and correlation coefficient (R^2) are given in Table 1. The value of "n" was utilized to represent the heterogeneous surface of the adsorbent. Results showed that adsorption of these metal ions obeyed Freundlich adsorption isotherm but adsorption of Ni(II) fitted well to Freundlich adsorption isotherm (R^2 > 0.99). The values of 'n' ranges from 2–10 shows good adsorption, 1–2 moderate adsorption and less than one represents poor sorption [28,44]. Moreover, adsorption of Ag(I) was higher whereas adsorption of Th(IV) and Ni(II) was moderate onto RH.

3.5. Adsorption kinetics

Herein, kinetic curves for adsorption of silver, thorium and nickel ions onto RH are represented in Fig. 6. Adsorption kinetics for these metal ions was studied by using the pseudo-first-order model and pseudo-second-order model.

Fig. 7 represents the plot of the pseudo-first-order model for adsorption of silver, thorium and nickel ions onto RH from aqueous solution. The calculated values of its endowments are given in Table 2. As shown in Table 2, the values of correlation coefficient (R^2) for Ag(I), Th(IV) and Ni(II) were 0.978, 0.991 and 0.765 respectively. There was a large difference between the values of the calculated adsorption capacity values ($q_{e,\text{cal}}$) and experimental adsorption capacity ($q_{e,\text{exp.}}$). From this, we can say that the pseudo-first-order model is not convenient to explain the rating process for adsorption of silver, thorium and nickel ions onto RH.

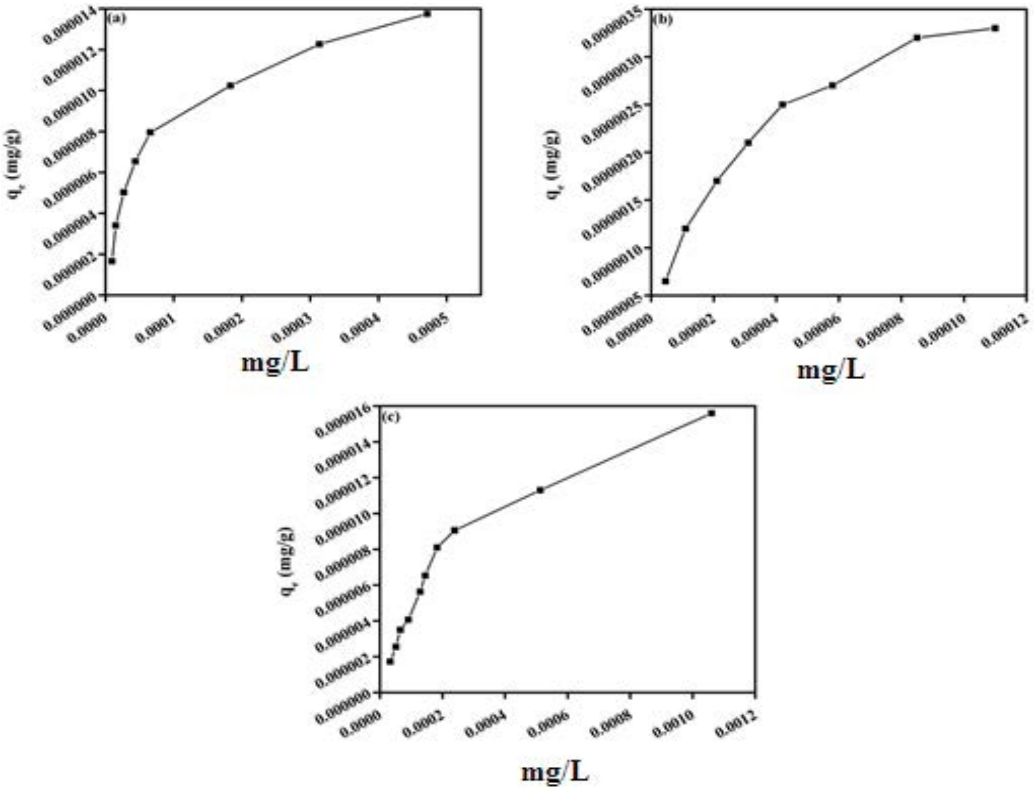

Fig. 3. Adsorption isotherm for adsorption of (a) Ag(I), (b) Th(IV), and (c) Ni(II) onto RH.

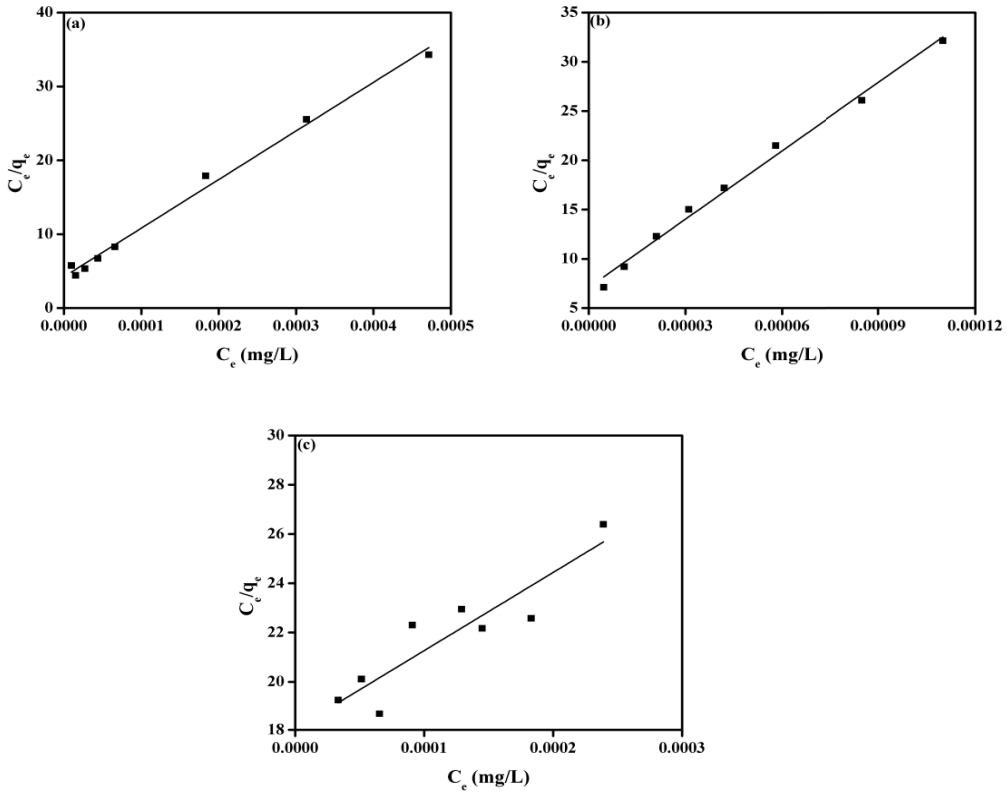

Fig. 4. Langmuir isotherm for adsorption of (a) Ag(I), (b) Th(IV), and (c) Ni(II) onto RH.

Table 1
Calculated parameters of Langmuir and Freundlich isotherms for adsorption of metal ions onto RH

Isotherm models		Parameters		
		Ag(I)	Th(IV)	Ni(II)
Langmuir isotherm	Q_m	1.52×10^{-5}	4.32×10^{-6}	3.15×10^{-5}
	K	15,479	32,573	1,754
	R^2	0.992	0.992	0.802
	R_L	0.053–0.411	0.129–0.571	0.163–0.778
Freundlich isotherm	K_F	6.11×10^{-4}	4.28×10^{-4}	1.21×10^{-2}
	n	2.11	1.93	1.17
	R^2	0.883	0.977	0.990

Q_m: mg/g; K_L: L/mol; K_F: mol/g.

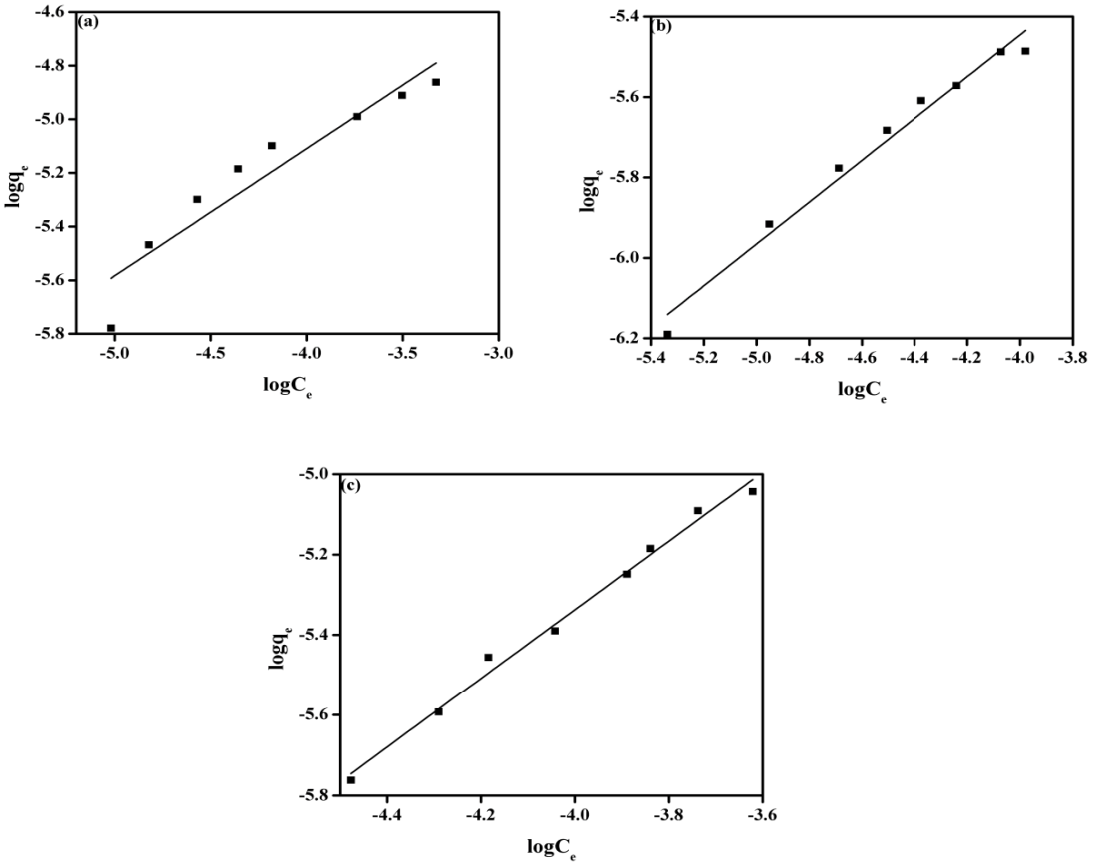

Fig. 5. Freundlich isotherm for adsorption of (a) Ag(I), (b) Th(IV), and (c) Ni(II) onto RH.

Fig. 8 depicts the plot of the pseudo-second-order model for adsorption of silver, thorium and nickel ions from aqueous solution onto RH. The determined values of its parameters are given in Table 2. It was observed that the values of calculated adsorption capacity for the entire metal ions (Ag(I), Th(IV) and Ni(II)) studied were in good agreement with experimental values. Moreover, the values of correlation coefficient (R^2) for the entire metal ions studied were close to unity. From this, we concluded that experimental data for adsorption of Ag(I), Th(IV) and Ni(II) onto RH fitted well to pseudo-second-order model.

3.6. Adsorption thermodynamics

Fig. 9 denotes the plots of $1/T$ vs. $\ln K_c$ for adsorption of silver, thorium and nickel ions from aqueous solution onto RH. The measured values of thermodynamic parameters ($\Delta H°$, $\Delta S°$, and $\Delta G°$) are given in Table 3. It was observed that the values of Gibb's free energy ($\Delta G°$) for adsorption of Ag(I), Th(IV) and Ni(II) onto RH were negative. It showed that adsorption of Ag(I), Th(IV) and Ni(II) onto RH was spontaneous in nature. With the increase in temperature, the decrease in values of Gibb's free energy denoted the

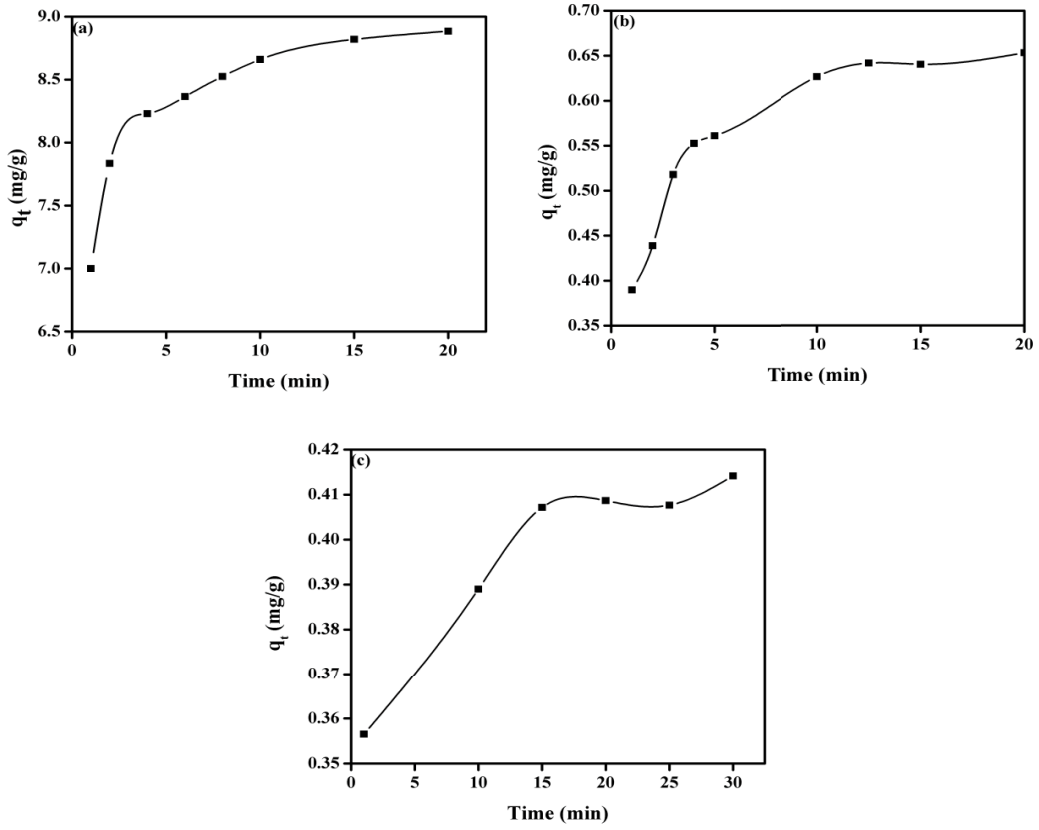

Fig. 6. The kinetic curve for adsorption of (a) Ag(I), (b) Th(IV), and (c) Ni(II) onto RH.

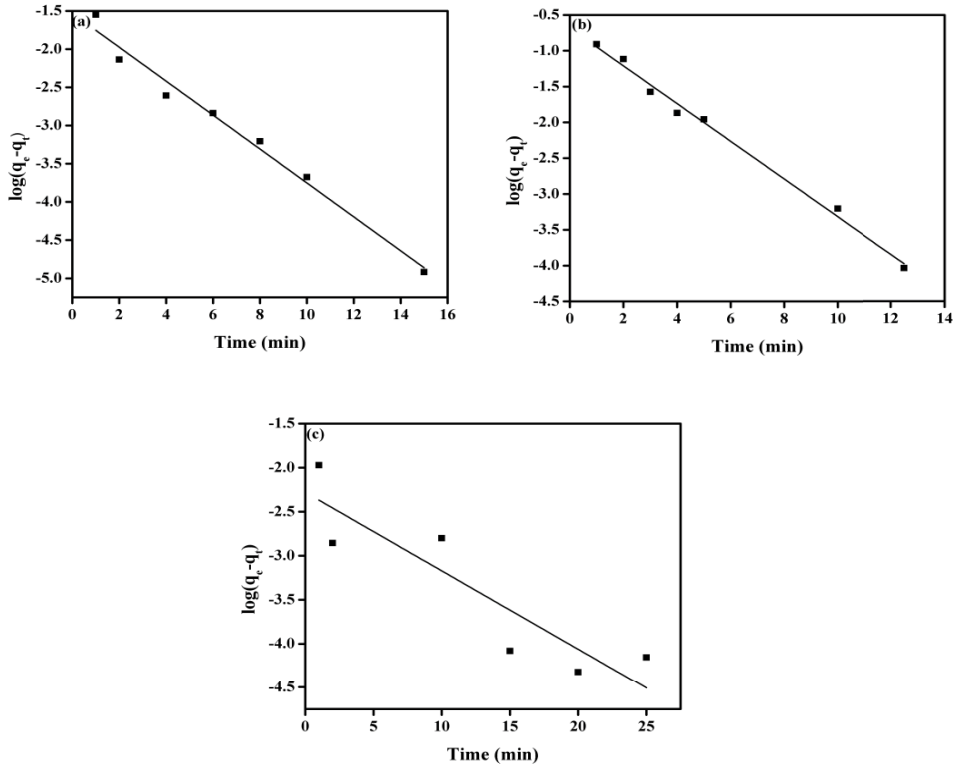

Fig. 7. Pseudo-first-order model for adsorption of (a) Ag(I), (b) Th(IV), and (c) Ni(II) onto RH.

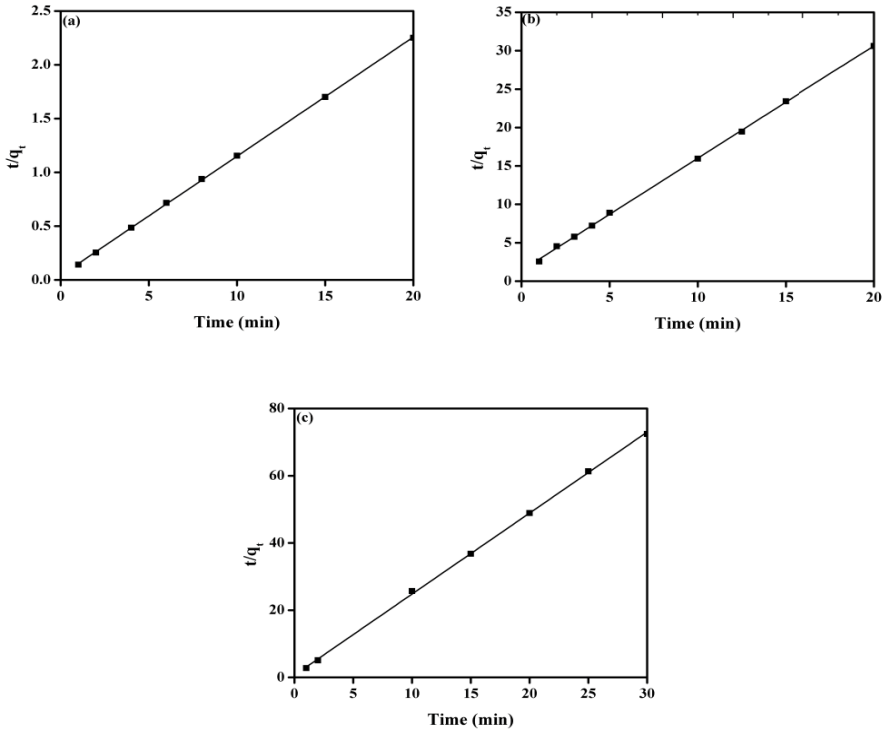

Fig. 8. Pseudo-second-order model for adsorption of (a) Ag(I), (b) Th(IV), and (c) Ni(II) onto RH.

Table 2
Determined adsorption kinetic parameters for adsorption of Ag(I), Th(IV) and Ni(II) onto RH

Kinetics models		Parameters		
		Ag(I)	Th(IV)	Ni(II)
Pseudo-first-order model	$q_{e,\text{exp.}}$	8.89	0.65	0.41
	q_e	0.029	0.21	0.81
	k_1	0.22	0.26	0.089
	R^2	0.978	0.991	0.765
Pseudo-second-order model	q_e	9.09	0.68	0.414
	k_2	0.29	1.54	8.47
	R^2	0.999	0.999	0.999

q_e: mg/g; k_1: (min^{-1}); k_2: g/mg min.

decline in the feasibility of the adsorption process at elevated temperatures. The attained positive value of entropy ($\Delta G°$) indicated the increase in randomness at the adsorbent–adsorbate interface during the adsorption of these metal ions onto RH from aqueous solution. Moreover, the positive value of enthalpy ($\Delta H°$) for adsorption of these metal ions onto RH showed that it was an endothermic process.

3.7. Regeneration of adsorbent (RH) and recovery of metal ions

For water treatment, the recovery of metal ions and regeneration of adsorbent is very important. A lot of efforts were made to regenerate RH by using HNO_3 solution of different molarities as desorbing media via batch mode. For specific intervals of time, a fixed quantity of metal-loaded RH was soaked into HNO_3 for recovery of these metal ions. Maximum recovery of silver ion (~60%) was attained by using 2.0 mol/L of HNO_3 solution whereas for thorium and nickel maximum recovery (~99%) was attained by employing 1.0 mol/L HNO_3 solution.

4. Conclusions

Herein, adsorption of Ag(I), Th(IV) and Ni(II) onto RH from aqueous solution was studied at ambient temperature. The successful adsorption of these metal ions onto RH was confirmed by FTIR and EDX studies. The percentage removal of Ag(I), Th(IV) and Ni(II) was increased from 73% to 92%, 40% to 68% and 43% to 60% respectively with contact time, 45% to 93%, 50% to 68% and 42% to 64% respectively with weight of RH and 94% to 96%, 61% to 81% and 60% to 65% respectively with temperature. Contrary, the percentage removal of Ag(I), Th(IV) and Ni(II) was decreased from 80% to 59%, 78% to 38% and 61% to 31% respectively with an initial concentration of the aqueous solution. With the pH of solution, the percentage discharge of Th(IV) and Ni(II) was enhanced from 11% to 80% and 6% to 63% respectively whereas decreased for Ag(I) from 79% to 56%. Results showed that adsorption of Ag(I) and Th(IV) onto RH fitted well to Langmuir isotherm whereas adsorption of Ni(II) onto RH fitted well to Freundlich isotherm because the value of correlation coefficient (R^2) was close to unity. The kinetic study demonstrated that adsorption of these metal ions onto RH obeyed the pseudo-second-order model because the value of correlation coefficient (R^2) was close to unity. Adsorption thermodynamics study exhibited that adsorption of these metal ions onto RH was an

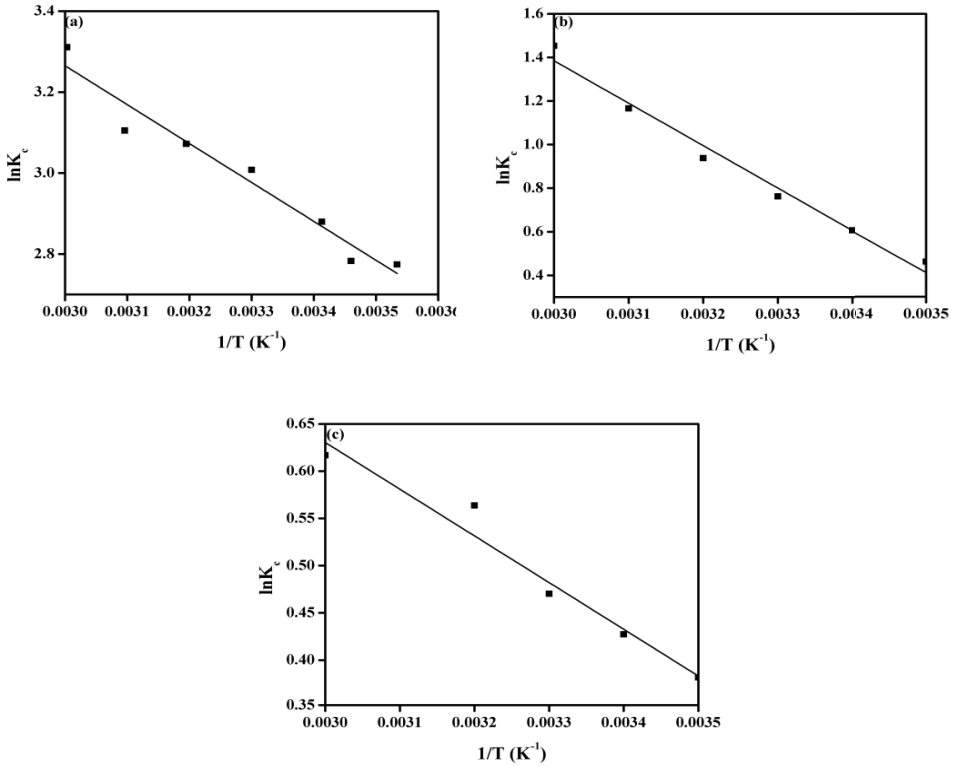

Fig. 9. The plot of $1/T$ vs. $\ln K_c$ for adsorption of (a) Ag(I), (b) Th(IV), and (c) Ni(II) onto RH.

Table 3
Calculated thermodynamic parameters for adsorption of Ag(I), Th(IV) and Ni(II) from aqueous solution onto RH

Temp. (K)		Ag(I)		Temp. (K)		Th(IV)		Temp. (K)		Ni(II)	
	$\Delta H°$	$\Delta S°$	$\Delta G°$		$\Delta H°$	$\Delta S°$	$\Delta G°$		$\Delta H°$	$\Delta S°$	$\Delta G°$
283.16			−6.53	288.16			−1.11	283.16			−0.89
289.16			−6.77	297.16			−1.50	293.16			−0.99
293.16			−7.02	303.16			−1.92	303.16	3.83	16.83	−1.06
303.16	7.99	51.02	−7.58	313.16	15.27	56.71	−2.44	313.16			−1.23
313.16			−7.99	323.16			−3.13	333.16			−1.40
323.16			−8.34	333.16			−3.57	–	–	–	–
333.16			−9.17	288.16			−1.11	–	–	–	–

ΔH: kJ/mol; ΔS: kJ/mol; ΔG: kJ/mol.

endothermic and spontaneous process. It is associated with the positive values of change in enthalpy ($\Delta H°$) and negative values of change in Gibb's free energy $\Delta G°$) for adsorption of these metal ions onto RH. Moreover, the maximum recovery of Ag(I) was attained by using 2.0 mol/L HNO_3 whereas 1.0 mol/L HNO_3 was used for maximum recovery for Th(IV) and Ni(II). It represented that RH could be utilized as an outstanding adsorbent for the discharge of Ag(I), Th(IV) and Ni(II) from the aqueous solution at room temperature.

Acknowledgment

The authors are highly thankful to Higher Education Commission (HEC), Pakistan for financial support.

References

[1] G. Boix, J. Troyano, L. Garzón-Tovar, C. Camur, N. Bermejo, A. Yazdi, J. Piella, N.G. Bastus, V.F. Puntes, I. Imaz, D. Maspoch, MOF-Beads containing inorganic nanoparticles for the simultaneous removal of multiple heavy metals from water, ACS Appl. Mater. Interfaces, 12 (2020) 10554–10562.
[2] L. Zhang, D. Peng, R.-P. Liang, J.-D. Qiu, Graphene-based optical nanosensors for detection of heavy metal ions, TrAC, Trends Anal. Chem., 102 (2018) 280–289.
[3] X. Qu, P.J.J. Alvarez, Q. Li, Applications of nanotechnology in water and wastewater treatment, Water Res., 47 (2013) 3931–3946.
[4] Jumina, Y. Priastomo, H.R. Setiawan, Mutmainah, Y.S. Kurniawan, K. Ohto, Simultaneous removal of lead(II), chromium(III), and copper(II) heavy metal ions through an adsorption process using C-phenylcalix[4]pyrogallolarene

material, J. Environ. Chem. Eng., 8 (2020) 103971, doi: 10.1016/j.jece.2020.103971.
[5] J. Wang, D. Zhang, S. Liu, C. Wang, Enhanced removal of chromium(III) for aqueous solution by EDTA modified attapulgite: adsorption performance and mechanism, Sci. Total Environ., 720 (2020) 137391, doi: 10.1016/j.scitotenv.2020.137391.
[6] T.A. Saleh, Nanocomposite of carbon nanotubes/silica nanoparticles and their use for adsorption of Pb(II): from surface properties to sorption mechanism, Desal. Water Treat., 57 (2015) 10730–10744.
[7] M.F. Hamza, S. Lu, K.A.M. Salih, H. Mira, A.S. Dhmees, T. Fujita, Y. Wei, T. Vincent, E. Guibal, As(V) sorption from aqueous solutions using quaternized algal/polyethyleneimine composite beads, Sci. Total Environ., 719 (2020) 137396, doi: 10.1016/j.scitotenv.2020.137396.
[8] X. Fang, J. Li, X. Li, S. Pan, X. Zhang, X. Sun, J. Shen, W. Han, L. Wang, Internal pore decoration with polydopamine nanoparticle on polymeric ultrafiltration membrane for enhanced heavy metal removal, Chem. Eng. J., 314 (2017) 38–49.
[9] W.A. Khanday, M. Asif, B.H. Hameed, Cross-linked beads of activated oil palm ash zeolite/chitosan composite as a bio-adsorbent for the removal of methylene blue and acid blue 29 dyes, Int. J. Biol. Macromol., 95 (2017) 895–902.
[10] K. Varaprasad, T. Jayaramudu, E.R. Sadiku, Removal of dye by carboxymethyl cellulose, acrylamide and graphene oxide via a free radical polymerization process, Carbohydr. Polym., 164 (2017) 186–194.
[11] Z. Yang, H. Yang, Z. Jiang, T. Cai, H. Li, H. Li, A. Li, R. Cheng, Flocculation of both anionic and cationic dyes in aqueous solutions by the amphoteric grafting flocculant carboxymethyl chitosan-graft-polyacrylamide, J. Hazard. Mater., 254–255 (2013) 36–45.
[12] B. Xiang, D. Ling, H. Lou, H. Gu, 3D hierarchical flower-like nickel ferrite/manganese dioxide toward lead(II) removal from aqueous water, J. Hazard. Mater., 325 (2017) 178–188.
[13] Y. Zhou, Y. He, Y. Xiang, S. Meng, X. Liu, J. Yu, J. Yang, J. Zhang, P. Qin, L. Luo, Single and simultaneous adsorption of pefloxacin and Cu(II) ions from aqueous solutions by oxidized multiwalled carbon nanotube, Sci. Total Environ., 646 (2019) 29–36.
[14] E. Erdem, N. Karapinar, R. Donat, The removal of heavy metal cations by natural zeolites, J. Colloid Interface Sci., 280 (2004) 309–314.
[15] J.C.Y. Ng, W.H. Cheung, G. McKay, Equilibrium studies of the sorption of Cu(II) ions onto chitosan, J. Colloid Interface Sci., 255 (2002) 64–74.
[16] R. Celis, M.C. HermosÍn, J. Cornejo, Heavy metal adsorption by functionalized clays, Environ. Sci. Technol., 34 (2000) 4593–4599.
[17] D. Sud, G. Mahajan, M.P. Kaur, Agricultural waste material as potential adsorbent for sequestering heavy metal ions from aqueous solutions – a review, Bioresour. Technol., 99 (2008) 6017–6027.
[18] M. Hua, S. Zhang, B. Pan, W. Zhang, L. Lv, Q. Zhang, Heavy metal removal from water/wastewater by nanosized metal oxides: a review, J. Hazard. Mater., 211–212 (2012) 317–331.
[19] I.S. Sayan Bhattacharya, A. Mukhopadhyay, D. Chattopadhyay, U.C. Ghosh, D. Chatterjee, Role of nanotechnology in water treatment and purification: potential applications implications, Int. J. Chem. Sci. Technol., 3 (2013) 59–64.
[20] S. Zafar, M.I. Khan, H. Rehman, J. Fernandez-Garcia, S. Shahida, P. Prapamonthon, M. Khraisheh, A. Rehman, H.B. Ahmad, M.L. Mirza, N. Khalid, M.H. Lashari, Kinetic, equilibrium, and thermodynamic studies for adsorptive removal of cobalt ions by rice husk from aqueous solution, Desal. Water Treat., 204 (2020) 285–296.
[21] G. Zhao, J. Li, X. Ren, C. Chen, X. Wang, Few-layered graphene oxide nanosheets as superior sorbents for heavy metal ion pollution management, Environ. Sci. Technol., 45 (2011) 10454–10462.
[22] O.S. Bello, O.M. Atoyebi, K.A. Adegoke, E.O. Fehintola, A.O. Ojo, Removal of toxicant chromium(VI) from aqueous solution using different adsorbents, J. Chem. Soc. Pak., 37 (2015) 190–206.
[23] U. Khalil, M.B. Shakoor, S. Ali, S.R. Ahmad, M. Rizwan, A.A. Alsahli, M.N. Alyemeni, Selective removal of hexavalent chromium from wastewater by rice husk: kinetic, isotherm and spectroscopic investigation, Water, 13 (2021) 263, doi: 10.3390/w13030263.
[24] R.K. Vempati, S.C. Musthyala, M.Y.A. Mollah, D.L. Cocke, Surface analyses of pyrolysed rice husk using scanning force microscopy, Fuel, 74 (1995) 1722–1725.
[25] S. Zafar, M.I. Khan, M. Khraisheh, S. Shahida,T. Javed, M.L. Mirza, N. Khalid, Use of rice husk as an efective sorbent for the removal of cerium ions from aqueous solution: kinetic, equilibrium and thermodynamic studies, Desal. Water Treat., 150 (2019) 124–135.
[26] S. Zafar, M.I. Khan, M. Khraisheh, S. Shahida, N. Khalid, M. Latif Mirza, Effective removal of lanthanum ions from aqueous solution using rice husk: impact of experimental variables, Desal. Water Treat., 132 (2019) 263–273.
[27] S. Zafar, M.I. Khan, M. Khraisheh, M.H. Lashari, S. Shahida, M.F. Azhar, P. Prapamonthon, M.L. Mirza, N. Khalid, Kinetic, equilibrium and thermodynamic studies for adsorption of nickel ions onto husk of *Oryza sativa*, Desal. Water Treat., 167 (2019) 277–290.
[28] S. Zafar, M.I. Khan, W. Hassan, S. Mubeen, T. Javed, S. Shahida, S. Manzoor, A. Shanableh, A. Rehman, M.L. Mirza, N. Khalid, M.H. Lashari, Application of NaOH-treated rice husk for adsorptive discharge of cobalt ions from wastewater, Desal. Water Treat., 226 (2021) 328–338.
[29] T.A. Saleh, Isotherm, kinetic, and thermodynamic studies on Hg(II) adsorption from aqueous solution by silica- multiwall carbon nanotubes, Environ. Sci. Pollut. Res. Int., 22 (2015) 16721–16731.
[30] V.K. Gupta, T.A. Saleh, Characterization of the chemical bonding between Al_2O_3 and nanotube in MWCNT/Al_2O_3 nanocomposite, Curr. Nanosci., 8 (2012) 739–743.
[31] U.C. Abubakar, K.R. Alhooshani, T.A. Saleh, Effect of ultrasonication and chelating agents on the dispersion of NiMo catalysts on carbon for hydrodesulphurization, J. Environ. Chem. Eng., 8 (2020) 103811, doi: 10.1016/j.jece.2020.103811.
[32] T.A. Saleh, Simultaneous adsorptive desulfurization of diesel fuel over bimetallic nanoparticles loaded on activated carbon, J. Cleaner Prod., 172 (2018) 2123–2132.
[33] T.A. Saleh, The influence of treatment temperature on the acidity of MWCNT oxidized by HNO_3 or a mixture of HNO_3/H_2SO_4, Appl. Surf. Sci., 257 (2011) 7746–7751.
[34] A. Rana, M.K. Arfaj, A.S. Yami, T.A. Saleh, Cetyltrimethylammonium modified graphene as a clean swelling inhibitor in water-based oil-well drilling mud, J. Environ. Chem. Eng., 8 (2020) 103802, doi: 10.1016/j.jece.2020.103802.
[35] V.C. Srivastaa, I.D. Mall, I.M. Mishra, Characterization of mesoporous rice husk ash (RHA) and adsorption kinetics of metal ions from aqueous solution onto RHA, J. Hazard. Mater., 134 (2006) 257–267.
[36] S. Kazy, K. Sar, P. Sen, A.K. Singh, F.D.S.S., Extracellular polysaccharides of a copper-sensitive and a copper-resistant *Pseudomonas aeruginosa* stain: synthesis, chemical nature and copper binding, World J. Microbiol. Biotechnol., 18 (2002) 583–588.
[37] S.K. Kazy, S. D'Souza, P. Sar, Uranium and thorium sequestration by a *Pseudomonas* sp.: mechanism and chemical characterization, J. Hazard. Mater., 163 (2009) 65–72.
[38] X. Ying-Mei, Q. Ji, H. De-Min, W. Dong-Mei, C. Hui-Ying, G. Jun, Z. Qiu-Min, Preparation of amorphous silica from oil shale residue and surface modification by silane coupling agent, Oil Shale, 27 (2010) 37–46.
[39] L. Ludueña, D. Fasce, V.A. Alvarez, P.M. Stefani, Nanocellulose from rice husk following alkaline treatment to remove silica, BioResources, 6 (2011) 1440–1453.
[40] S. Larous, A.-H. Meniai, M.B. Lehocine, Experimental study of the removal of copper from aqueous solutions by adsorption using sawdust, Desalination, 185 (2005) 483–490.
[41] A. Özer, D. Özer, A. Özer, The adsorption of copper(II) ions on to dehydrated wheat bran (DWB): determination of the

equilibrium and thermodynamic parameters, Process Biochem., 39 (2004) 2183–2191.
[42] J. Egila, B. Dauda, T. Jimoh, Biosorptive removal of cobalt(II) ions from aqueous solution by *Amaranthus hydridus* L. stalk wastes, Afr. J. Biotechnol., 9 (2010) 8192–8198.
[43] M. Malakootian, A. Almasi, H. Hossaini, Pb and Co removal from paint industries effluent using wood ash, Int. J. Environ. Sci. Technol., 5 (2008) 217–222.
[44] B. Subramanyam, A. Das, Linearized and non-linearized isotherm models comparative study on adsorption of aqueous phenol solution in soil, Int. J. Environ. Sci. Technol., 6 (2009) 633–640.

Supporting information

S1. Adsorption of silver, thorium and nickel onto rice husk

In a typical procedure, a known amount of rice husk (RH) was taken into a 25 cm^3 secured cap culture tube along with 4 cm^3 of standard acid solution and a fixed quantity of stock radiotracer with a known quantity of Ag(I), Th(IV) and Ni(II) solutions were added. Continuously, the contents were equilibrated on a wrist-action mechanical shaker (Vibromatic, USA) at a rate of 500 rpm for specific intervals of time. Then, it was centrifuged at 5,000 rpm for phase separation and the supernatant solution was withdrawn for activity measurement. The radioactivity of solutions before (A_i) and after (A_f) equilibrium was recorded with a NaI well-type scintillation counter (Canberra Inc., United States of America (USA)) coupled with a counter-scaler (Nuclear Chicago). A volume of 1.0 cm^3 was normally used to measure the activity. All experiments were performed at ambient temperature. The percentage discharge of Ag(I), Th(IV) and Ni(II) by RH from an aqueous solution were determined by the following equation:

$$\%\ \text{adsorption} = \frac{A_i - A_f}{A_i} \times 100 \tag{S1}$$

where A_i and A_f show initial and final adsorption of metal ions (counts/min) into solution respectively.

Batch desorption of silver ion was carried out by using 2.0 mol/L HNO_3 solution whereas for thorium and nickel ions was used 1.0 mol/L of HNO_3 solution as a desorbing media for 5 min.

Fig. S1. Rice husk of basmati rice.

S2. Instrumentations

Field emission scanning electron microscope (FE-SEM, SIRION 200, FEI Company, USA) was used to study the morphology of RH before and after adsorption of metal ions. Fourier transform infrared (FTIR) spectrum of RH was taken by attenuated total reflectance (ATR) with FTIR spectrometer (Vector 22, Bruker) having a resolution of 2 cm^{-1} and total spectral range of 4,000–400 cm^{-1} before and after adsorption of metal ions. Successful adsorption of silver, thorium and nickel ions onto RH was also demonstrated by energy-dispersive X-ray analysis.

S3. Adsorption equilibrium

S3.1. Langmuir adsorption isotherm

The linearized form of Langmuir adsorption isotherm is given as [1]:

$$\frac{C_e}{q_e} = \frac{1}{Q_m K_L} + \frac{C_e}{Q_m} \tag{S2}$$

where Q_e (mg of adsorbate per g of adsorbent) is the adsorption density at the equilibrium solute concentration C_e. C_e is the equilibrium concentration of adsorbate in solution (mg/L). Q_m (mg of solute adsorbed per g of adsorbent) is the maximum adsorption capacity corresponding to complete monolayer coverage. K_L is the Langmuir constant related to the energy of the adsorption (L of adsorbate per mg of adsorbent).

An essential feature of a Langmuir isotherm can be expressed in terms of a dimensionless constant 'separation factor' parameter, 'R_L' that is used to predict if an adsorption system is "favorable" or "unfavorable" and can be expressed as follows:

$$R_L = \frac{1}{\left(1 + k_L C_o\right)} \tag{S3}$$

where C_o is the initial concentration of metal ions (mol/L) and K_L is the Langmuir sorption equilibrium constant (L/mol). The value of R_L indicates the adsorption process to be either unfavorable ($R_L > 1$), linear ($R_L = 1$), favorable ($0 < R_L < 1$) or irreversible ($R_L = 0$).

S3.2. Freundlich adsorption isotherm

The linearized form of Freundlich adsorption isotherm is expressed as [S1]:

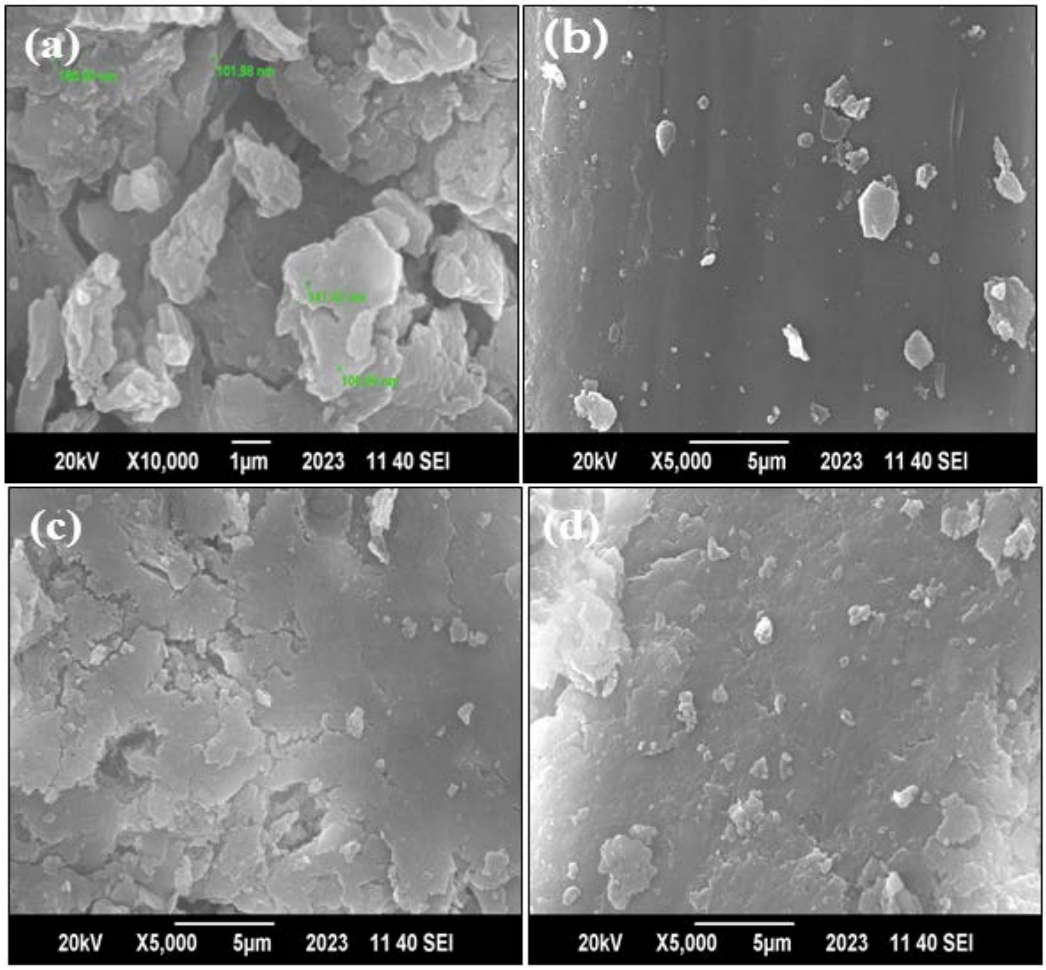

Fig. S2. FE-SEM image of (a) virgin RH, (b) Ag(I) loaded RH, (c) Th(IV) loaded RH, and (d) Ni(II) loaded RH.

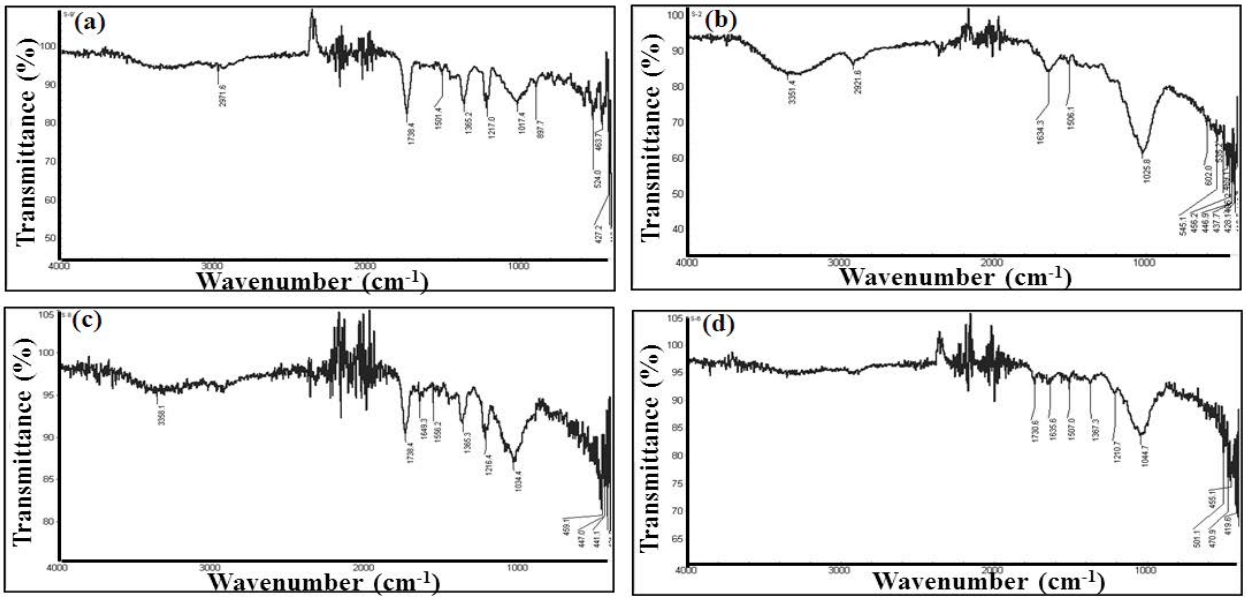

Fig. S3. FTIR spectrum of (a) virgin RH, (b) Ag(I) loaded RH, (c) Th(IV) loaded RH, and (d) Ni(II) loaded RH.

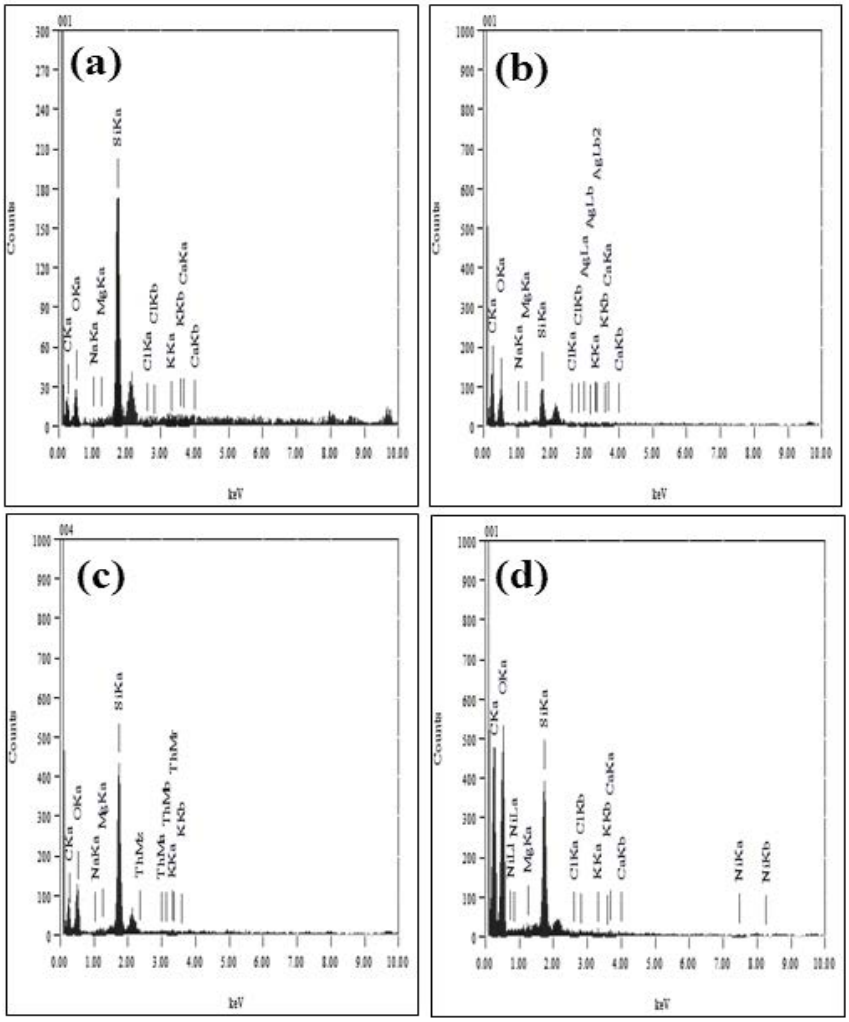

Fig. S4. Energy-dispersive X-ray image of (a) virgin RH, (b) Ag(I) loaded RH, (c) Th(IV) loaded RH, and (d) Ni(II) loaded RH.

$$\log q_e = \log k_f + \frac{1}{n}\log C_e \tag{S4}$$

where Q_e is the quantity of solute adsorbed at equilibrium (adsorption density: mg of adsorbate per g of adsorbent). C_e is the concentration of adsorbate at equilibrium, where K_F and $1/n$ are empirical constants dependent on the nature of sorbent and sorbate and the temperature.

S4. Adsorption kinetics

S4.1. Pseudo-first-order model

The Lagergren pseudo-first-order rate in linear form is represented as [S2–S4]

$$\log\left(q_e - q_t\right) = \log q_e - \frac{K_1 t}{2.303} \tag{S5}$$

where k_1 (/min), q_e and q_t are rate constant of pseudo-first-order model, the concentration of metal ion solution adsorbed at equilibrium and time t respectively.

S4.2. Pseudo-second-order model

The pseudo-second-order kinetic model linearized form is represented as [S2,S3,S5]:

$$\frac{t}{q_t} = \frac{1}{k_2 q_e^2} + \frac{t}{q_e} \tag{S6}$$

where k_2 (g/mg min) is the rate constant of pseudo-second-order model.

References

[S1] J.N. Nsami, J.K. Mbadcam, The adsorption efficiency of chemically prepared activated carbon from cola nut shells by $ZnCl_2$ on methylene blue, J. Chem., 2013 (2013) 1–7.
[S2] M.I. Khan, A. Shanableh, J. Fernandez, M.H. Lashari, S. Shahida, S. Manzoor, S. Zafar, A. ur Rehman, N. Elboughdiri, Synthesis of DMEA-grafted anion exchange membrane for adsorptive discharge of methyl orange from wastewaters, Membranes, 11 (2021) 166, doi: 10.3390/membranes11030166.
[S3] M.I. Khan, M.H. Lasahri, M. Khraisheh, S. Shahida, S. Zafar, P. Prapamonthon, A. Rehman, S. Anjum, N. Akhtar, F. Hanif, Adsorption kinetic, equilibrium and thermodynamic studies of

Eosin-B onto anion exchange membrane, Desal. Water Treat., 155 (2019) 84–93.
[S4] M.I. Khan, T.M. Ansari, S. Zafar, A.R. Buzdar, M.A. Khan, F. Mumtaz, P. Prapamonthon, M. Akhtar, Acid green-25 removal from wastewater by anion exchange membrane: adsorption kinetic and thermodynamic studies, Membr. Water Treat., 9 (2018) 79–85.
[S5] M.A. Khan, M.I. Khan, S. Zafar Removal of different anionic dyes from aqueous solution by anion exchange membrane, Membr. Water Treat., 8 (2017) 259–277.